International Journal of Bifurcation and Chaos

HIDDEN AND NON-STANDARD BIFURCATION DIAGRAM OF AN ALTERNATE QUADRATIC SYSTEM

G. PASTOR[1], M. ROMERA[1], M.-F. DANCA[2], A. MARTIN[1], A.B. ORUE[1], F. MONTOYA[1], L. HERNÁNDEZ ENCINAS[1]

[1]*Instituto de Tecnologías Físicas y de la Información (ITEFI)*
Consejo Superior de Investigaciones Científicas (CSIC)
Serrano 144, Madrid, 28006, Spain
{*gerardo, miguel, agustin, amalia.orue, fausto, luis*}*@iec.csic.es*

[2]*Dept. of Mathematics and Computer Science,*
Emanuel University of Oradea,
410597 Oradea, România.
Also at Romanian Institute of Science and Technology,
Cireşilor 29, Cluj-Napoca, 400487, România.
danca@rist.ro

Received (to be inserted by publisher)

Alternate quadratic systems A: $x_{n+1} = \begin{cases} 1-ax_n^2, \text{ if } n \text{ is even} \\ 1-a_*x_n^2, \text{ if } n \text{ is odd} \end{cases}$ and B: $x_{n+1} = \begin{cases} 1-a_*x_n^2, \text{ if } n \text{ is even} \\ 1-ax_n^2, \text{ if } n \text{ is odd} \end{cases}$, where a and a_* are different parameters, seem to be interval maps in a range of the parameter values. However, after a careful graphical analysis of their bifurcation diagrams we conclude that this is true only for system B, but not for system A. In System A we find a hidden and non-standard bifurcation diagram ("hidden" because it is not visible at normal resolution and "non-standard" because the bifurcation diagram is empty for some ranges of the parameter values). The different behavior of the underlying critical polynomial in the range of parameter values in both alternate quadratic systems explains why the hidden and non-standard bifurcation diagram is present in system A and not in system B. The analysis of the Lyapunov exponent also shows both the existence and the different behavior of the hidden bifurcation diagram of system A.

Keywords: Nonlinear dynamics; nonlinear discrete dynamical systems; quartic maps; alternate quadratic system; hidden and non-standard bifurcation diagrams.

1. Introduction

The seasonal behavior of many natural phenomena can be modeled as a switching between different environmental conditions. Thus, Maier and Peacock-López [2010] iterate the quadratic logistic map by switching the parameter from a first value when the iteration is odd to a second value when the iteration is even.

Let $C(I,I)$ be the class of continuos functions that map the unit interval $I=[0,1]$ into itself. Given two maps f and g in $C(I,I)$, the alternating system

$$x_{n+1}=\begin{cases} f(x_n), & \text{if } n \text{ is even,} \\ g(x_n), & \text{if } n \text{ is odd,} \end{cases}$$

has been studied from a general point of view [D'Aniello & Steele, 2011; D'Aniello & Oliveira, 2009]. Danca et *al.* [2008] use a periodic or random switching scheme of the bifurcation parameter in order to integrate a continuous-time dynamical system, of integer or fractional order.

Recently, the alternate iteration of the quadratic map $x_{n+1}=1-ax_n^2$ is used, where the parameter takes alternatively the values a and a_* according to the systems

$$\text{A}:\ x_{n+1}=\begin{cases} 1-ax_n^2, & \text{if } n \text{ is even,} \\ 1-a_*x_n^2, & \text{if } n \text{ is odd,} \end{cases} \tag{1}$$

and

$$\text{B}:\ x_{n+1}=\begin{cases} 1-a_*x_n^2, & \text{if } n \text{ is even,} \\ 1-ax_n^2, & \text{if } n \text{ is odd,} \end{cases} \tag{2}$$

that are named alternate quadratic systems A and B [Romera *et al.*, 2015].

As seen there, the orbits of the alternate quadratic systems A and B can be obtained by adding the orbits of the quartic maps $x_{n+1}=1-a\left(1-a_*x_n^2\right)^2$ and $x_{n+1}=1-a_*\left(1-ax_n^2\right)^2$ (different approaches to the iteration of quartic maps can be seen in [Jánosi & Gallas, 1999; Gallas, 1993, 1994, 1995]).

Continuing our work Romera *et al.* [2015], in this paper we show that only system B is a map of the interval. Indeed, in system B any orbit belonging to the range of parameter values $R_p=[a_1,a_3]$ is bounded while any orbit outside $R_p=[a_1,a_3]$ goes to infinity. However, in system A, we can find orbits outside $R_p=[a_1,a_3]$ that do not go to infinity. In this paper we analyze system A in such a zone outside the range $R_p=[a_1,a_3]$. In order to undertake this purpose, we begin by first seeing the alternate iteration of a quadratic map. Next, by starting from the graphical analysis of five little points found outside of the range $R_p=[a_1,a_3]$ on the bifurcation diagram of system A, we find out a hidden and non-standard bifurcation diagram ("hidden" because it is not visible at a resolution of $\Delta a=1\text{E}-3$, used in figures presented in [Romera *et al.*, 2015], and "non-standard" because the bifurcation diagram is empty for some ranges of the parameter values). Then, the analysis of the critical polynomials helps us to better understand why the hidden and non-standard bifurcation diagram is present in system A and not in system B. To finish, the analysis of the Lyapunov exponent confirms both previous analysis, that of the bifurcation diagram and that of the critical polynomials. Indeed, the Lyapunov exponent also shows both the existence and the different nature of the hidden bifurcation diagram in system A.

2. Alternate iteration of a quadratic map

As is well known, any orbit of a one-dimensional quadratic map depending on a parameter is a map of the interval I when the orbit is bounded. This occurs for a range of parameter values R_p; outside R_p, the orbit always goes to infinity (*map of the interval I in* R_p).

The bifurcation diagrams of two quadratic maps, $x_{n+1}=1-ax_n^2$ and $x_{n+1}=x_n^2+c$, are shown in Fig. 1. The extremes of the range of parameter values R_p for these two maps are T and $\text{M}_{2,1}$. The values of T are: $a=-0.25$ and $c=0.25$, and the values of $\text{M}_{2,1}$ are: $a=2$ and $c=-2$. Hence, the range of parameter values R_p for these two maps are: $R_{p_a}=[-0.25,2]$ and $R_{p_c}=[-2,0.25]$. As can be seen in [Romera *et al.*, 2015], outside these ranges, the orbits of the critical points escape to infinity and, inside the range, the orbits do not escape, as expected, and are inside the interval $I_a=[-1,2]$ and $I_c=[-2,2]$, respectively.

In literature, the range of parameter values R_p of the logistic map, $x_{n+1}=\lambda x_n(1-x_n)$, is assumed to be $R_p=[1,4]$ and the interval of the orbit values $I=[0,1]$ (see Fig. 2(a)). However, in the logistic map case R_p range becomes: $R_{p_\lambda}=[-2,4]$. Indeed, as can be seen in Fig. 2(b), the bifurcation diagram has two parts, each one in a well-defined range of parameter values: $R_{p_\lambda}=R_{p_1}\cup R_{p_2}=[-2,4]$, where $R_{p_1}=[-2,1]$

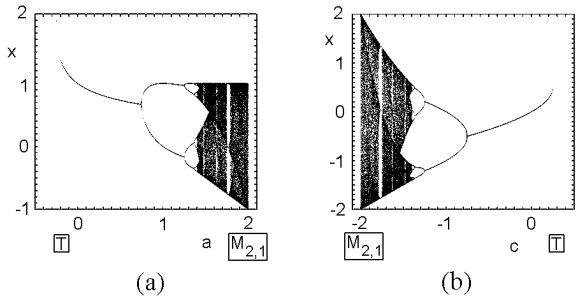

Fig. 1. Bifurcation diagrams of two quadratic maps showing the location of the points T and $M_{2,1}$. (a) $x_{n+1} = 1 - ax_n^2$ and (b) $x_{n+1} = x_n^2 + c$.

and $R_{p_2} = [1, 4]$. Nevertheless, these two parts are topologically conjugate [Grossmann & Thomae, 1977; Milnor & Thurston, 1988], and then equivalent. Hence, we will continue to consider the logistic map as a map of the interval $I = [0, 1]$ in $R_p = [1, 4]$ since from a topological point of view it is the same. Only from this point of view can be considered the statement "Note that a quadratic map only has one parameter value causing a point T and one parameter value causing a point $M_{2,1}$" of Section 3 of [Romera *et al.*, 2015]. Indeed, as can be seen in Fig. 2(b), in the complete representation there are two parameter values ($\lambda = -2$ and $\lambda = 4$) causing a point $M_{2,1}$.

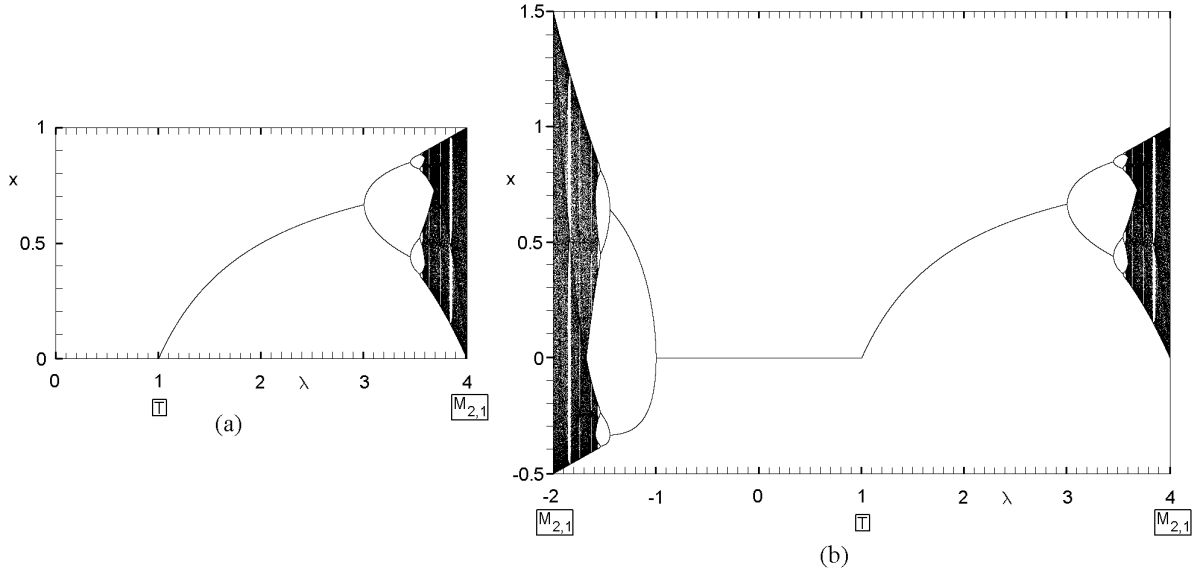

Fig. 2. Bifurcation diagram of the logistic map $x_{n+1} = \lambda x_n(1 - x_n)$ showing the location of the points T and $M_{2,1}$. (a) Standard representation. (b) Complete representation.

Since all the one-dimensional quadratic maps are topologically conjugate [Grossmann & Thomae, 1977; Milnor & Thurston, 1988], it is enough to study one of them. Hence, from now on we only work with the following one: $x_{n+1} = 1 - ax_n^2$. Starting from this map, let us consider the systems (1) and (2).

Now, let us introduce two quartic maps:

$$\mathrm{C} : x_{n+1} = 1 - a(1 - a_* x_n^2)^2$$

and

$$\mathrm{D} : x_{n+1} = 1 - a_*(1 - a x_n^2)^2.$$

The following evident conclusion can be found in [Romera *et al.*, 2015]:

Property: *The orbit of the critical point* 0 of *the alternate quadratic system* A(B) *can be obtained by superposing the orbit of the critical value* 1 *of the quartic map* C(D) *with the orbit of the critical point* 0 *of the quartic map* D(C).

That is to say, the dynamics of an alternate quadratic system can also be obtained from the dynamics of quartic maps.

In Fig. 3 (also Fig. 3 in [Romera *et al.*, 2015]) the bifurcation diagrams of the systems A and B are shown when we fix the parameter $a_* = 1.754877$ and we vary the parameter a. In accordance with the last Property, the bifurcation diagram of the system A can also be obtained by the superposition of the bifurcation diagrams of the quartic C (initial point $x_0 = 1$) and the quartic D (initial point $x_0 = 0$); likewise, the bifurcation diagram of the system B can be obtained by the superposition of the bifurcation diagrams of the quartic C (initial point $x_0 = 0$) and the quartic D (initial point $x_0 = 1$), as can be seen in Fig. 4 (also Fig. 4 in [Romera *et al.*, 2015]).

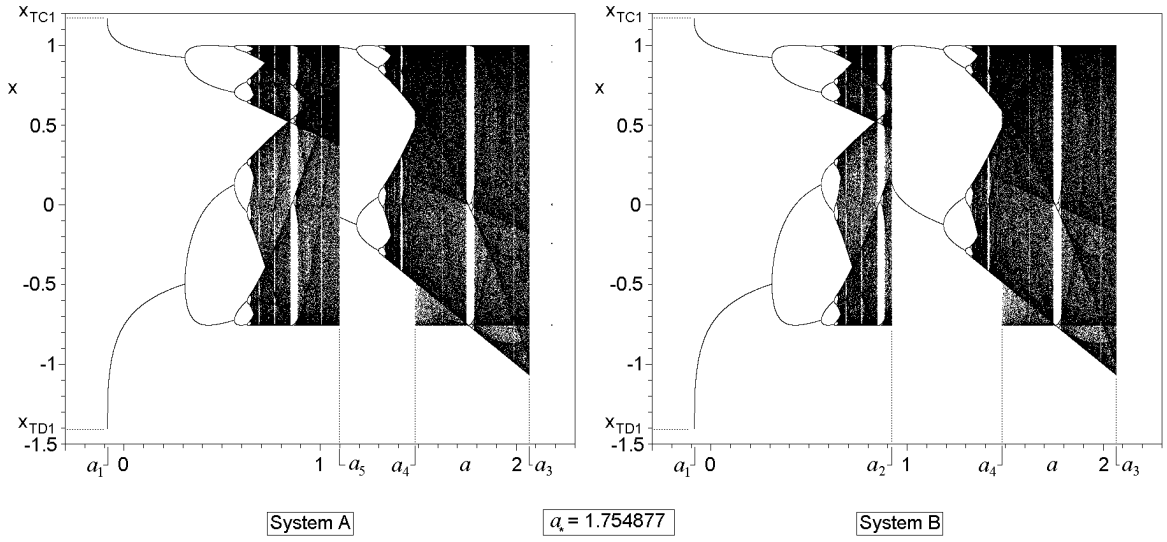

Fig. 3. Bifurcation diagrams of systems A and B when $a_* = 1.754877$.

As shown in detail in [Romera *et al.*, 2015], the breaking points by tangency (T points) and by pre-periodicity ($M_{m,n}$ points) can be obtained with no problem. In the case at hand, when $a_* = 1.754877$, all these breaking points (a_1, a_2, a_3, a_4 and a_5, in Figs. 3 and 4) are carefully analyzed in both systems A and B. As it is said there, in both systems if $a < a_1 = -0.086457$ and $a > a_3 = 2.067558$ the orbits escape to infinity (in this paper we are going to see the exceptions), while if $a > a_1$ and $a < a_3$ the orbit does not escape to infinity, always belonging to the interval $I = [x_{TD1}, x_{TC1}]$. Therefore, the alternate quadratic systems A and B seemed to be maps of the interval $I = [x_{TD1}, x_{TC1}]$ in $R_p = [a_1, a_3]$.

3. Five small points on the bifurcation diagram of system A

We wonder if the five points almost imperceptibles observed in the bifurcation diagram of system A (which do not seem to be present in system B), Fig. 3 near $a \sim 2.18$, are artifacts. In [Romera *et al.*, 2015] it is shown that there is at least one orbit that does not escape to infinity outside the range $[a_1, a_3]$, and hence we cannot properly say that both systems A and B are maps of the interval $I = [x_{TD1}, x_{TC1}]$ in the range of parameter values $R_p = [a_1, a_3] = [-0.086457, 2.067558]$. Therefore, we should extend the range of parameter values outside $R_p = [a_1, a_3]$.

In the following sections, first we are going to analyze the bifurcation diagrams in the extended range of parameter values. Next, we shall analyze the critical polynomials in this new range of parameter values,

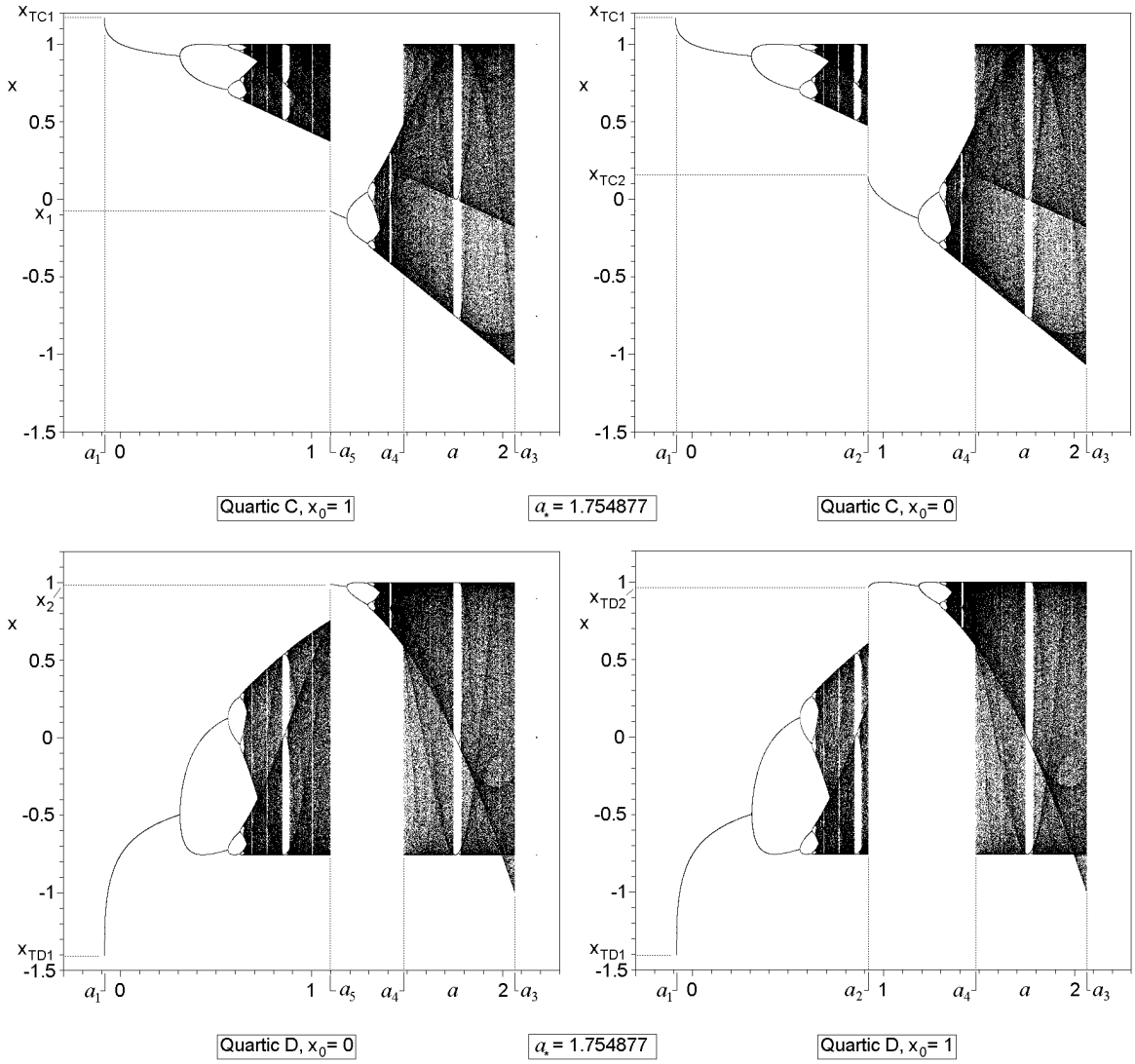

Fig. 4. Bifurcation diagrams of quartics C and D, with initial points $x_0 = 0$ and $x_0 = 1$, when $a_* = 1.754877$.

and finally we shall analyze the Lyapunov exponent in the same extended range.

4. Bifurcation diagram in the extended range of parameter values

As indicated before, if we see the bifurcation diagrams of Fig. 3, at first glance both systems A and B indeed seem to be maps of the interval I in the range of parameter values $R_p = [a_1, a_3]$. However, due to the presence of the five small points outside $R_p = [a_1, a_3]$ in system A, we will extend the range of parameter values beyond $R_p = [a_1, a_3]$ up to a new range to be determined.

Let us consider a graphical analysis of system A. For this purpose we amplify the almost imperceptible five points of the bifurcation diagram for the parameter value $a \sim 2.18$. Clearly, we do not have enough precision in Fig. 3 to locate the points. Therefore, we have to find these points by trial and error. After having located these points, they have been amplified as seen in Fig. 5. At first glance, it seems that every point has become a small and perfect bifurcation diagram. Therefore we should have a zone of period 5. However, the point of the bottom has become two superposed bifurcation diagrams; hence, there are six bifurcation diagrams in total and period 6.

Will there be more groups of tiny points like the five points found for $a \sim 2.18$ for other parameter values? As suspected, by increasing the parameter value beyond 2.3, which is the limit of Fig. 3, there are

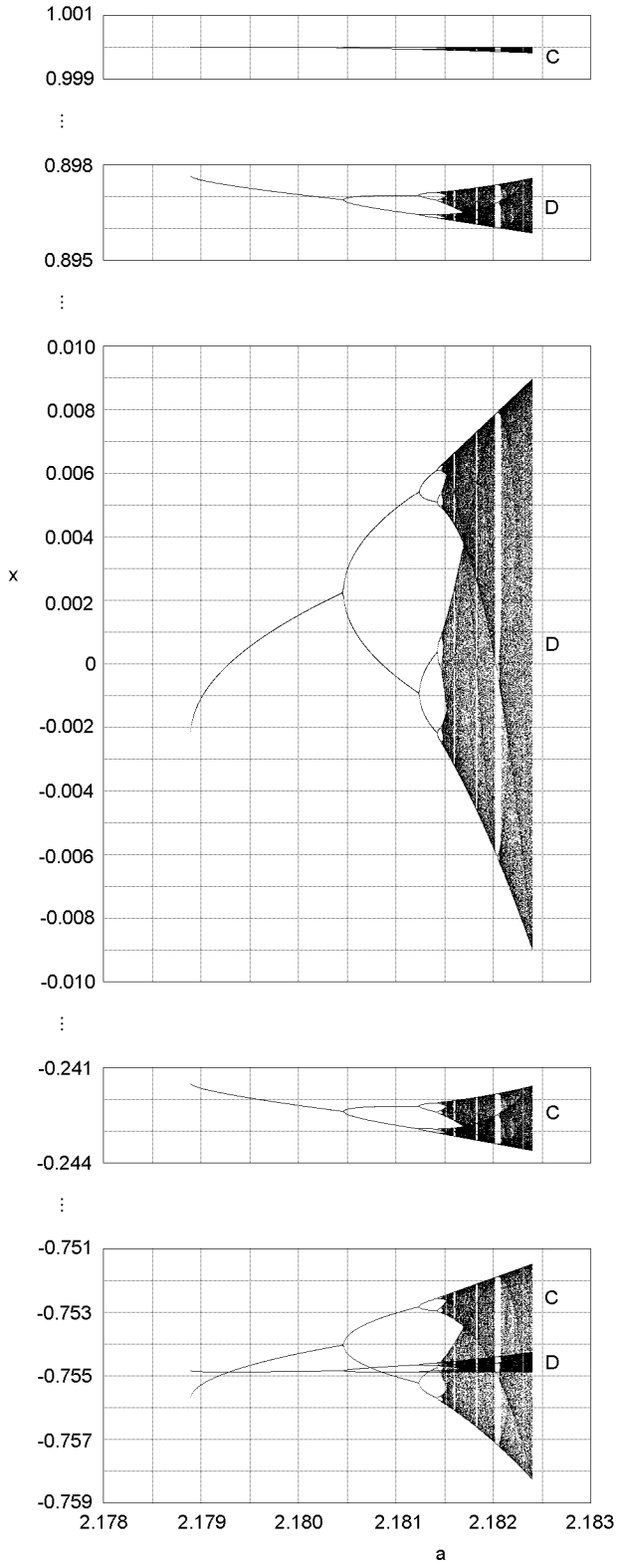

Fig. 5. Zoom in the neighborhood of $a \sim 2.18$ for each one of the little points of System A. Each point becomes a small bifurcation diagram, except that of the bottom that becomes two.

several more groups of tiny points, e.g. for parameter values $a \sim 2.87, a \sim 3.08, \ldots$ In all these cases, the tiny points become perfect tiny bifurcation diagrams when they are amplified.

What we have just seen shows that system A has orbits that do not escape to infinity for values of the parameter outside the range $R_p = [a_1, a_3]$. Having reached this point, we have the following question: if we work with more resolution, is there a hidden bifurcation diagram in which the orbits of system A are bounded in the range $R_p^h = [a_3, a_6]$, where $a_6 > a_3$, a_6 being a parameter to be determined? If so, system A would still be a map of the interval I, now in the extended range $R_p^e = [a_1, a_6]$. The bifurcation diagram in the range $[a_3, a_6]$ could be called *hidden bifurcation diagram* since it is practically hidden when it is drawn with normal resolution.

To answer to our question let us focus again on Fig. 3, where bifurcation diagrams of systems A and B are shown when we fix the parameter $a_* = 1.754877$ and we vary the parameter a from $a = -0.3$ to $a = 2.3$. As shown in this figure and said before, system B seems indeed a map of the interval $I = [x_{TD1}, x_{TC1}]$ in $R_p = [a_1, a_3]$. However, system A is not a map of the interval $I = [x_{TD1}, x_{TC1}]$ in $R_p = [a_1, a_3]$ because, beyond a_3, there are points of the parameter a which do not escape to infinity.

In Fig. 6 we show the bifurcation diagram of the system A but now the parameter varies from $a = -0.2$ to $a = 3.7$. Fig. 6 has been drawn with the same resolution used for Fig. 3, e. g. both figures have been drawn with the same increase of the parameter: $\Delta a = 1\mathrm{E} - 3$. For this resolution, three groups of tiny points, each group for the same a, can be seen. The first one, with apparent period 5, corresponding to a parameter value $a \sim 2.18$, is the group of five tiny points of Fig. 3. The other two groups, of apparent periods 6 and 3, correspond to parameter values $a \sim 2.87$ and $a \sim 3.08$. As has been pointed out before, all these tiny points become perfect tiny bifurcation diagrams when they are amplified.

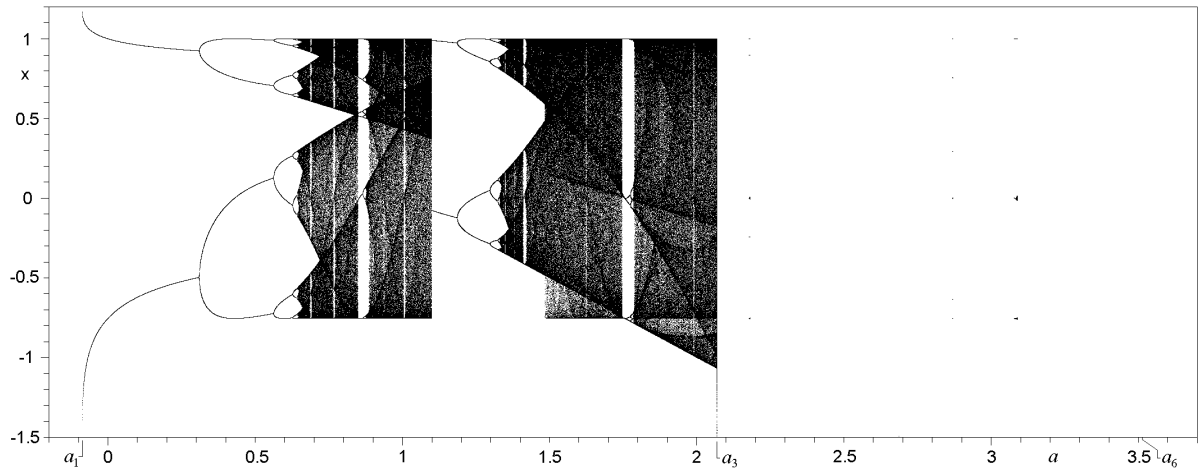

Fig. 6. Bifurcation diagram of System A of Fig. 3 with the same resolution but with an extended range of parameter values $R_p^e = [a_1, a_6]$.

Figure 6 shows two very different regions. The first one in the range of parameter values $[-0.086457, 2.067558]$ ($R_p = [a_1, a_3]$ in Fig. 3) which we call visible region of the diagram, and the second one in the range of parameter values $[a_3, a_6]$, where a_6 is a parameter value to be determined, that we call hidden region. Obviously, if we want the hidden region of the diagram can be seen, we have to increase the resolution.

When we successively improve resolution from $\Delta a = 1\mathrm{E} - 3$ to $\Delta a = 1\mathrm{E} - 4$, $\Delta a = 1\mathrm{E} - 5$ and so on, the resulting figures show more and more details (see Fig. 7, where the case of $\Delta a = 1\mathrm{E} - 9$ is presented). Beyond this resolution it is very tedious to draw new figures and no important improvement is observed in them.

Hence, Fig. 7 has been drawn with an increase of the parameter $\Delta a = 1\mathrm{E} - 9$ instead of $\Delta a = 1\mathrm{E} - 3$ of the Fig. 6. As expected, the visible region has essentially the same information in both figures. Let us compare now the hidden region in both figures.

The hidden region of Fig. 6 has only three groups of tiny points. However, the hidden region of Fig. 7 presents two characteristics. First, straight lines that are a continuation of those of the visible region, and

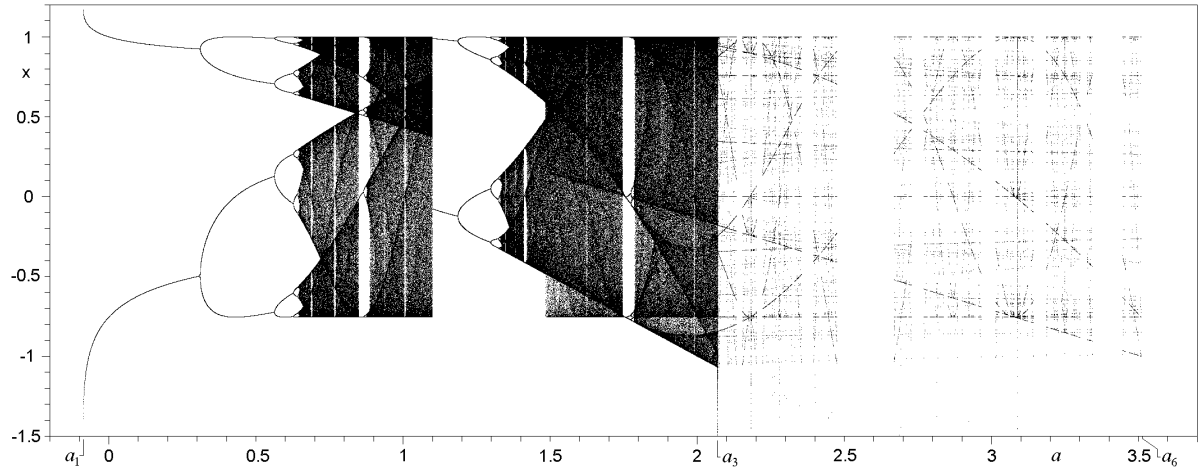

Fig. 7. The same Fig. 6 but with more resolution (increase of the parameter $\Delta a = 1\mathrm{E}-9$ instead of $\Delta a = 1\mathrm{E}-3$ of the Fig. 6).

curves that are a continuation of the curves of the critical polynomials of the visible region can clearly be seen. Therefore, in accordance with the first characteristic, the hidden region seems to be the continuation of the bifurcation diagram of the visible region.

Second, there is another notable characteristic of this hidden region: for some ranges of the parameter, such as $[2.47502, 2.66966]$, the bifurcation diagram is empty, i.e., the orbits escape to infinity in this range. Hence, the hidden region of the diagram is not a map of the interval $I = [x_{TD1}, x_{TC1}]$ in $R_p^h = [a_3, a_6]$; and, therefore, it is not a standard bifurcation diagram. However, as said before, it seems to be a prolongation of the bifurcation diagram of the visible region. That is why we can call it non-standard bifurcation diagram; and, since it is also a hidden diagram, we can finally call it *hidden and non-standard bifurcation diagram.*

In the same way that some breaking points (a_1, a_2, a_3, a_4 and a_5, in Fig. 3 and Fig. 4) are calculated in the visible region in [Romera *et al.*, 2015], it is also possible to calculate a_6, the upper limit of the range of parameter values of this hidden and non-standard bifurcation diagram in the hidden region. For this purpose let us focus here on breaking points by instability.

Let us consider the quartic C: $f_{\mathrm{C}}(x) = 1 - a(1 - a_* x^2)^2$, whose critical points are 0 and $\pm(1/a_*)^{1/2}$ and whose critical values are $1-a$ and 1. The orbit of the critical point 0 is: 0, $1-a$, $f_{\mathrm{C}}(1-a)$, $f_{\mathrm{C}}[f_{\mathrm{C}}(1-a)]\ldots$, and the orbit of the critical value 1 is: 1, $f_{\mathrm{C}}(1)$, $f_{\mathrm{C}}[f_{\mathrm{C}}(1)]\ldots$. By taking into account these two orbits, several cases can be studied as can be seen in [Romera *et al.*, 2015]. However, in order to calculate a_6 we are going to focus our attention only on the following case.

Let us start from the orbit of the critical value 1, and let us consider the case $f_{\mathrm{C}}(1) = f_{\mathrm{C}}[f_{\mathrm{C}}(1)]$, corresponding to a Misiurewicz point $\mathrm{M}_{1,1}$. When a_* = constant, the equation $f_{\mathrm{C}}(1) = f_{\mathrm{C}}[f_{\mathrm{C}}(1)]$ has five solutions. Ignoring the trivial solution $a = 0$ (double) we have

$$a = 2/(1 - a_*)^2 \tag{3}$$

and

$$a = \left[1 \pm (-1 + 2/a_*)^{1/2}\right] / (1 - a_*)^2 \, . \tag{4}$$

The solution of Eq. (3) (Eq. (16) in [Romera *et al.*, 2015]) is $a_6 = 3.509762$, which corresponds to the value graphically determined by zooming enough the upper limit of the hidden region.

To finish this section, let us see now system B. Fig. 8 shows the bifurcation diagram of system B of Fig. 3 but now for the extended range of parameter values $R_p^e = [a_1, a_6]$. As can clearly be seen in the figure, in this case there is no hidden bifurcation diagram. Hence, at the contrary of system A, system B not only seems but indeed is a map of the interval $I = [x_{TD1}, x_{TC1}]$ in $R_p = [a_1, a_3]$.

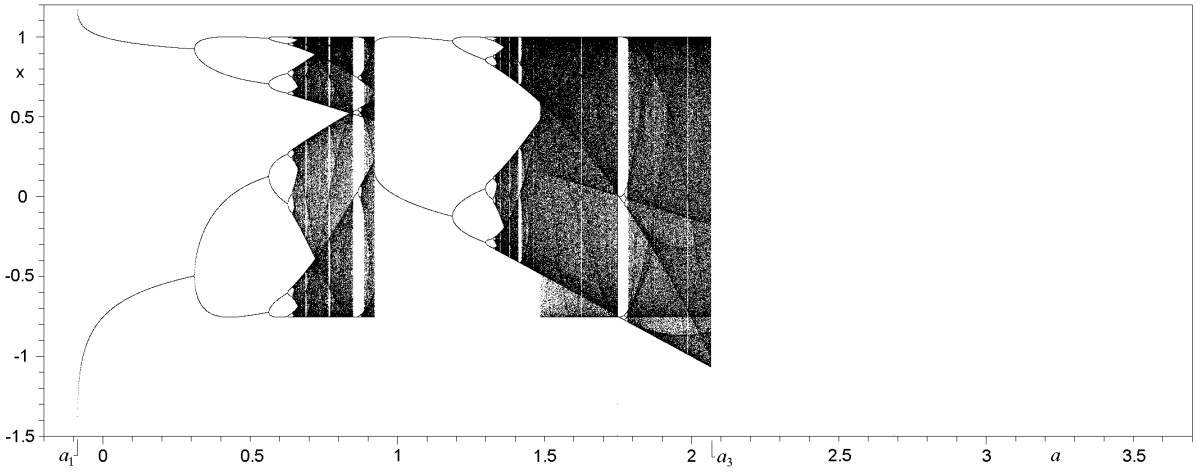

Fig. 8. Complete bifurcation diagram of system B when $x_0 = 0$ and $a_* = 1.754877$.

5. Critical polynomials

Zeng et *al.* [1984] defined a dynamical system of polynomials which are now called critical polynomials. They are the skeleton of the bifurcation diagram of a map depending on a parameter $x_{n+1} = f(\mu, x_n)$, and their intersections are the superstable orbits. Critical polynomials are $P_{n+1} = f(\mu, P_n)$, where $P_0 = x_0$, and x_0 is an initial value (a critical point or a critical value) giving superstable orbits. We are going to analyze critical polynomials in both system A and system B in order to strengthen our study of the hidden region.

Let us see firstly system B which is equivalent to the superposition of quartic C with $x_0 = 0$ and quartic D with $x_0 = 1$.

The critical polynomials of the quartic C: $x_{n+1} = 1 - a\big(1 - a_* x_n^2\big)^2$, where $a_* = 1.754877$, $x_0 = 0$ (critical point) and a is the parameter, are: $P_{n+1} = 1 - a\big(1 - a_* P_n^2\big)^2$, where $P_0 = 0$. That is to say:

$$\begin{aligned} P_0 =& 0 \,, \\ P_1 =& 1 - a \,, \\ P_2 =& 1 - a\left[1 - a_*(1-a)^2\right]^2 \,, \\ & \cdots \end{aligned}$$

Figure 9 shows the critical polynomials $P_0, P_1, P_2, \ldots, P_5$ of the quartic C: $x_{n+1} = 1 - a\big(1 - a_* x_n^2\big)^2$, when $a_* = 1.754877$ and $x_0 = 0$.

Likewise, Fig. 10 shows the critical polynomials $P_0, P_1, P_2, \ldots, P_5$ of the quartic D: $x_{n+1} = 1 - a_*\big(1 - a x_n^2\big)^2$, when $a_* = 1.754877$ and $x_0 = 1$.

In order to analyze these two figures, let us take into account that the parameter value corresponding to a superstable orbit of period p is the solution of the equation

$$P_p = P_0 \,. \tag{5}$$

Likewise, the parameter value corresponding to a Misiurewicz point $\mathrm{M}_{n,m}$ is the solution of

$$P_n = P_{n+m}. \tag{6}$$

That is to say, the parameter values corresponding to superstable orbits and Misiurewicz points correspond to intersections of critical polynomials.

If we focus on Fig. 9, where the critical polynomials $P_0, P_1, P_2 \ldots, P_5$ of the quartic C: $x_{n+1} = 1 - a\big(1 - a_* x_n^2\big)^2$, when $a_* = 1.754877$ and $x_0 = 0$ are shown, we can see that, for $a > a_3$, $P_2, P_3, P_4, \ldots$ take values more and more negative. In this case of $a > a_3$, there is no intersection of P_0 with $P_1, P_2, \ldots$ (no

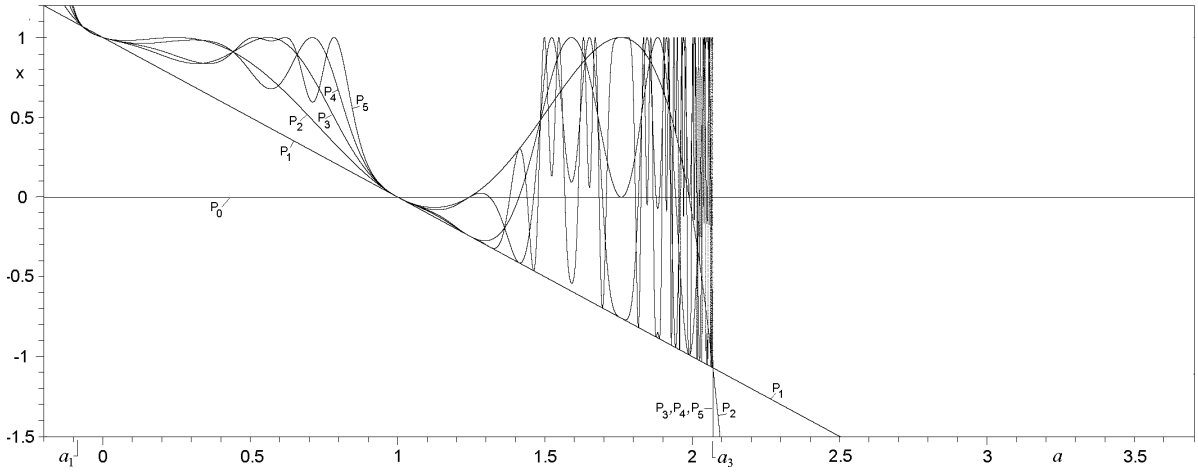

Fig. 9. Critical Polynomials $P_0, P_1, P_2, \ldots, P_5$ of quartic C: $x_{n+1} = 1 - a\left(1 - a_* x_n^2\right)^2$, when $a_* = 1.754877$ and $x_0 = 0$.

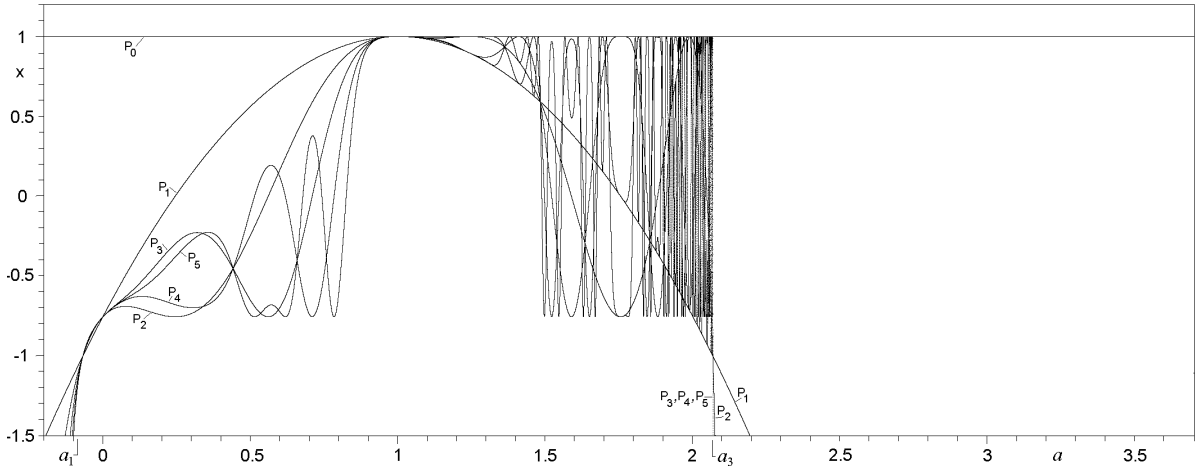

Fig. 10. Critical polynomials $P_0, P_1, P_2, \ldots, P_5$ of quartic D: $x_{n+1} = 1 - a_*\left(1 - a x_n^2\right)^2$, when $a_* = 1.754877$ and $x_0 = 1$.

superstable orbit) or between $P_1, P_2, \ldots$ (no Misiurewicz point). Hence, for $a > a_3$ there is no hidden bifurcation diagram. The same behavior can be seen in Fig. 10, where the critical polynomials $P_0, P_1, P_2 \ldots, P_5$ of this quartic D: $x_{n+1} = 1 - a_* \left(1 - a x_n^2\right)^2$, when $a_* = 1.754877$ and $x_0 = 1$ are shown. Again, for $a > a_3$ there is no hidden bifurcation diagram. Therefore, system B, which is equivalent to the superposition of quartic C with $x_0 = 0$ and quartic D with $x_0 = 1$ previously seen, has no hidden bifurcation diagram either.

Let us see now system A which is equivalent to the superposition of quartic C with $x_0 = 1$ and quartic D with $x_0 = 0$.

The critical polynomials of the quartic C: $x_{n+1} = 1 - a\left(1 - a_* x_n^2\right)^2$, where $a_* = 1.754877$, $x_0 = 1$

(critical value) and a is the parameter, are: $P_{n+1} = 1 - a\big(1 - a_* P_n^2\big)^2$, where $P_0 = 1$. That is to say:

$$
\begin{aligned}
&P_0 = 1\ ,\\
&P_1 = 1 - a(1 - a_*)^2,\\
&P_2 = 1 - a\Big[1 - a_*\Big[1 - a(1 - a_*)^2\Big]^2\Big]^2,\\
&P_3 = 1 - a\Bigg[1 - a_*\Bigg[1 - a\Big[1 - a_*\Big[1 - a(1 - a_*)^2\Big]^2\Big]^2\Bigg]^2\Bigg]^2,\\
&\dots
\end{aligned}
$$

Figure 11 shows the critical polynomials $P_0, P_1, P_2 \dots, P_5$ of this quartic C: $x_{n+1} = 1 - a\big(1 - a_* x_n^2\big)^2$, when $a_* = 1.754877$ and $x_0 = 1$.

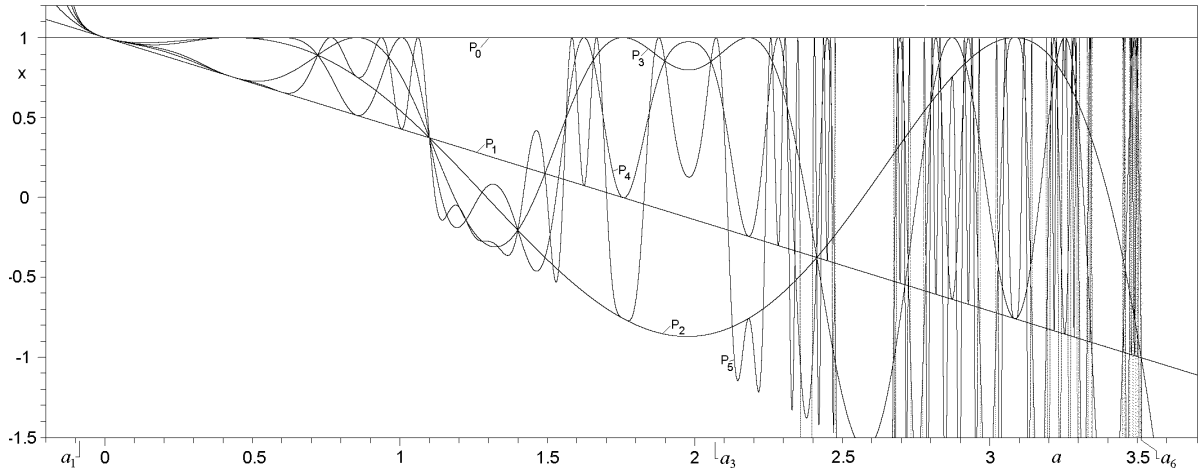

Fig. 11. Critical polynomials $P_0, P_1, P_2 \dots, P_5$ of quartic C: $x_{n+1} = 1 - a\Big(1 - a_* x_n^2\Big)^2$, when $a_* = 1.754877$ and $x_0 = 1$.

The critical polynomials of the quartic D: $x_{n+1} = 1 - a_*\big(1 - a x_n^2\big)^2$, where $a_* = 1.754877$, $x_0 = 0$ (critical point) and a is the parameter, are: $P_{n+1} = 1 - a_*\big(1 - a P_n^2\big)^2$, where $P_0 = 0$. That is to say:

$$
\begin{aligned}
&P_0 = 0\ ,\\
&P_1 = 1 - a_*,\\
&P_2 = 1 - a_*\Big[1 - a(1 - a_*)^2\Big]^2,\\
&P_3 = 1 - a_*\Bigg[1 - a\Big[1 - a_*\Big[1 - a(1 - a_*)^2\Big]^2\Big]^2\Bigg]^2,\\
&\dots
\end{aligned}
$$

Figure 12 shows the critical polynomials $P_0, P_1, P_2 \dots, P_5$ of the quartic D: $x_{n+1} = 1 - a_*\big(1 - a x_n^2\big)^2$, when $a_* = 1.754877$ and $x_0 = 0$.

As can be seen in both Figs. 11 and 12, when $a > a_3$ there are a lot of intersections of P_0 with $P_1, P_2, \dots$ or between $P_1, P_2, \dots$. Hence, in System A there is an extended range of parameter values where critical polynomials intersect, what means that for $a > a_3$ there is a hidden bifurcation diagram.

Let next see if there are some sub-ranges of the parameter where there is no intersection (if so, in these sub-ranges the bifurcation diagram will be empty). As can be seen in Figs. 11 and 12, none of the critical polynomials $P_0, P_1, P_2 \dots, P_5$ intersect in some sub-ranges, $[2.47502, 2.66966]$ being the most

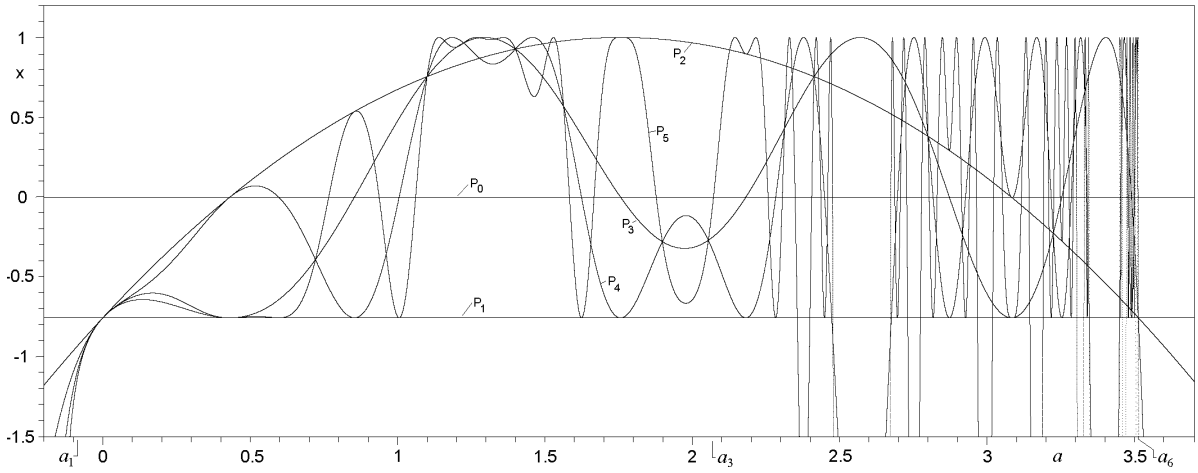

Fig. 12. Critical polynomials $P_0, P_1, P_2 \ldots, P_5$ of quartic D: $x_{n+1} = 1 - a_*\left(1 - ax_n^2\right)^2$, when $a_* = 1.754877$ and $x_0 = 0$.

obvious. Since quartic C: $x_{n+1} = 1 - a\left(1 - a_* x_n^2\right)^2$, when $a_* = 1.754877$ and $x_0 = 1$; and quartic D: $x_{n+1} = 1 - a_*\left(1 - ax_n^2\right)^2$, when $a_* = 1.754877$ and $x_0 = 0$ have the same sub-ranges without intersections, we shall use only the first one but now with one hundred critical polynomials for a better vision of these sub-ranges (see Fig. 13).

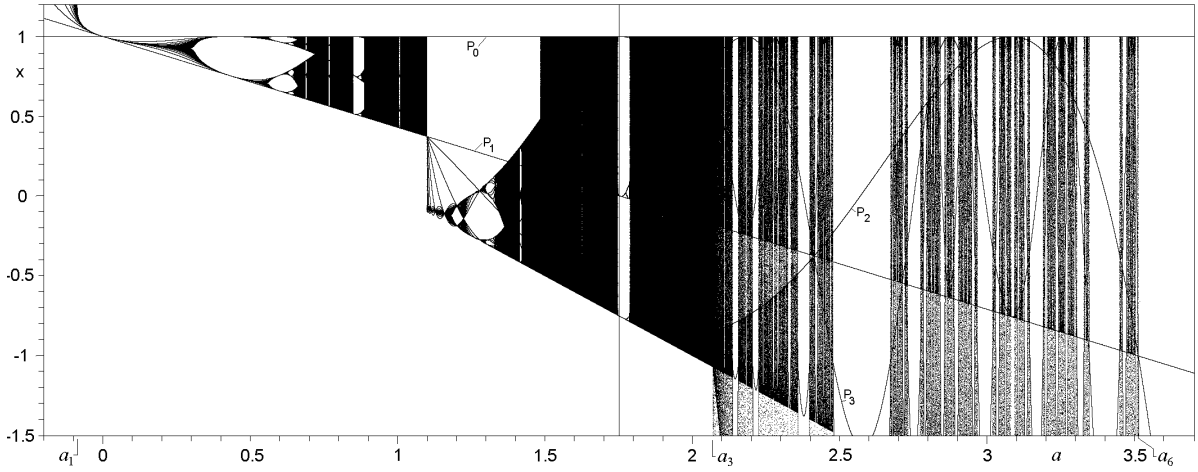

Fig. 13. Critical polynomials $P_0, P_1, P_2, \ldots, P_{99}$ of quartic C: $x_{n+1} = 1 - a\left(1 - a_* x_n^2\right)^2$, when $a_* = 1.754877$ and $x_0 = 1$.

The former results highlight the existence in system A of a hidden and non-standard bifurcation diagram, as shown in the above section.

6. Lyapunov exponent of an alternate quadratic system

Let us carry out a new graphical analysis by using the Lyapunov exponent. As is well known, in one-dimensional quadratic maps there are three types of points according to the value of the Lyapunov exponent Λ: points where $\Lambda < 0$ (stable and superstable periodic points), points where $\Lambda = 0$ (bifurcations points), and points where $\Lambda > 0$ (Misiurewicz points). Next, we determine the values of Λ of an alternate quadratic system.

In the case of a one-dimensional map depending on a parameter, $x_{n+1} = f(\mu, x_n)$, Shaw [1981] gives

the following expression to calculate the Lyapunov exponent:

$$\Lambda(\mu) = \lim_{N\to\infty} \frac{1}{N} \sum_{n=0}^{N-1} \ln \left| f'(\mu, x_n) \right|. \tag{7}$$

Hence, the Lyapunov exponent of an alternate system $x_{n+1} = \begin{cases} f_1(\mu, x_n), & \text{if } n \text{ is even (odd)}, \\ f_2(\mu, x_n), & \text{if } n \text{ is odd (even)}, \end{cases}$ can be obtained by means of

$$\Lambda(\mu) = \frac{1}{N} \sum_{n=0}^{N-1} \left[\ln \left| f_1'(\mu, x_n) \right| + \ln \left| f_2'(\mu, x_n) \right| \right]. \tag{8}$$

Let us begin by applying Eq. (8) to calculate the Lyapunov exponent of system A when $a_* = 1.754877$ and a is a variable. The Lyapunov exponent of system A will be $\Lambda(a) = \frac{1}{N} \sum_{n=0}^{N-1} \ln \left| -2 \left(a x_{2n} + a_* x_{2n+1} \right) \right|$ and is shown in Fig. 14(a).

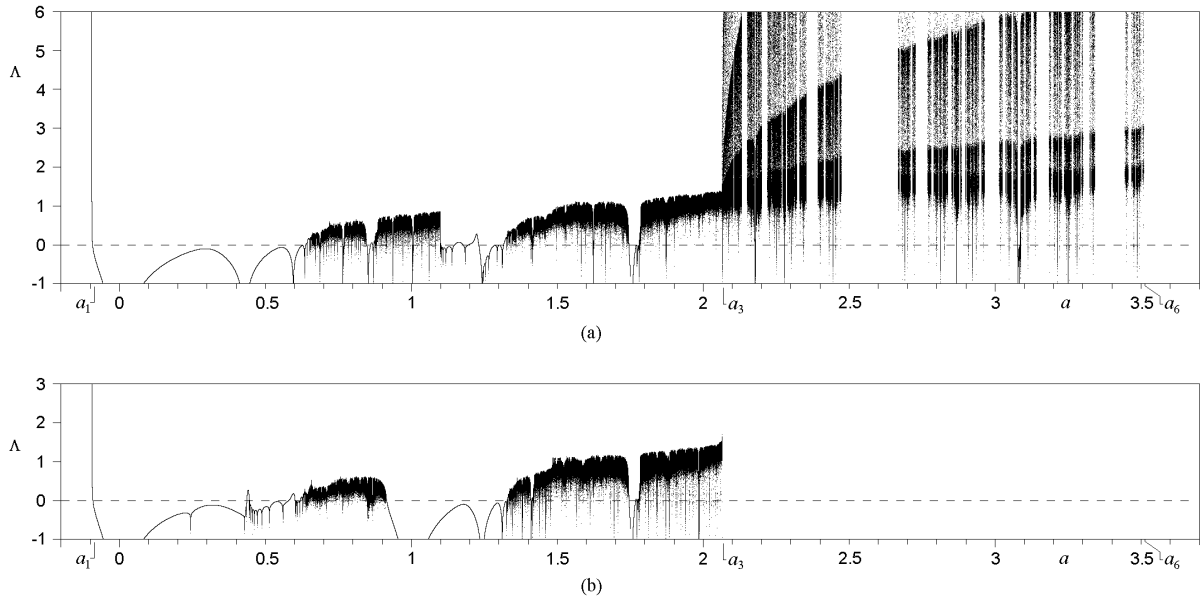

Fig. 14. (a) Lyapunov exponent of system A. (b) Lyapunov exponent of system B. ($a_* = 1.754877$. $N = 1000$ and $\Delta a = 1\text{E}{-6}$ if $a \leq a_3$; $N = 20$ and $\Delta a = 1\text{E} - 7$ if $a > a_3$).

Figure 14(a) shows again two very different regions: the first one in the range of parameter values $[a_1, a_3]$ which is the equivalent to the visible region, and the second one in the range of parameter values $[a_3, a_6]$ which is the equivalent to the hidden region. In Fig. 14(a) both regions are perfectly visible. The first region is similar to the Lyapunov exponent of a one-dimensional quadratic map [Pastor *et al.*, 1997].

Let us analyze the Lyapunov exponent of the second region. We can verify the existence of the same empty zones for the same ranges of the parameter. If for example, in Fig. 7 the range of parameter values $[2.47502, 2.66966]$ is empty, because the orbits escape to infinity, this same range is empty in Fig. 14(a) because Λ also escapes to infinity. This fact corroborates the conclusions of the former Sections 4 and 5 and shows that Λ has a non-standard behavior in the hidden region.

Let us note the different values of Λ in the range $[a_1, a_3]$, which corresponds to the visible region, and in the range $[a_3, a_6]$ which corresponds to the hidden region. In $[a_1, a_3]$ the values of Λ have a boundary clearly lesser than those of $[a_3, a_6]$. Indeed, Λ is always bounded by 2 in the first case. However, the boundary of Λ is much greater than 6 (limit of the figure) in the second case, according to Fig. 14(a), what indicates a much more chaotic behavior.

Let us apply now Eq. (8) to calculate the Lyapunov exponent of system B when $a_* = 1.754877$, and a is a variable. The Lyapunov exponent of system B will be $\Lambda(a) = \frac{1}{N}\sum_{n=0}^{N-1} \ln|-2\,(a_* x_{2n} + a x_{2n+1})|$ and is shown in Fig. 14(b). This figure has been drawn again with $N = 1000$ iterations and an increase of the parameter $\Delta a = 1\text{E}-6$ if $a \leq a_3$, and with $N = 20$ iterations and an increase of the parameter $\Delta a = 1\text{E}-7$ if $a > a_3$.

In Fig. 14(b) only the range of parameter values $[a_1, a_3]$ has finite values of Λ. There is no figure for $a > a_3$. Hence in system B there is no hidden region.

Therefore, the analysis of the Lyapunov exponent confirms what we pointed out in Sections 4 and 5, and shows that only system A has a non-standard region in the range of parameter values $[a_3, a_6]$.

7. Conclusions

Amplifying the almost imperceptible five points of the bifurcation diagram of system A for a parameter value $a \sim 2.18$, every point becomes one small and perfect bifurcation diagram (in some cases one point can correspond to more than one bifurcation diagram).

After zooming once and again, we can see a bifurcation diagram in a new range of parameter values, $R_p^h = [a_3, a_6]$, that could be called hidden bifurcation diagram since it is practically hidden when it is drawn with normal resolution.

The hidden bifurcation diagram seems to be a prolongation of the bifurcation diagram of the visible region, because both the straight lines and the curves of the critical polynomials are the continuation of those of the visible region.

The hidden bifurcation diagram is empty for some sub-ranges of $R_p^h = [a_3, a_6]$. Hence, the hidden bifurcation diagram is not a true map of the interval $I = [x_{TD1}, x_{TC1}]$ in $R_p^h = [a_3, a_6]$ and, therefore, we call it a non-standard bifurcation diagram. Then, we have found a hidden an non-standard bifurcation diagram.

We can find a_6 both graphically (by zooming) and analytically. Likewise, we can find it analytically as a solution of Eq. (3) that calculates some breaking points in the bifurcation diagram.

By studying the critical polynomials of quartics C: $x_{n+1} = 1 - a\big(1 - a_* x_n^2\big)^2$ and D: $x_{n+1} = 1 - a_*\big(1 - a x_n^2\big)^2$, we can see a hidden and non-standard bifurcation diagram in system A and not in system B.

A graphical analysis of the Lyapunov exponent shows us that the same sub-ranges of parameter values which are empty in the hidden bifurcation diagram are also empty now.

The different values of Λ in the visible region, where Λ is always bounded by 2, and in the hidden region, where the boundary of Λ is much greater than 6, indicate a much more chaotic behavior in this hidden region.

Acknowledgments

This research was partially supported by both Ministerio de Economía y Competitividad (Spain) under project ProCriCis, reference TIN2014-55325-C2-1-R, and Comunidad de Madrid (Spain) under project reference S2013/ICE-3095-CIBERDINE-CM.

References

Danca, M.-F., Tang, W. K. S. & Chen, G. [2008] "A switching scheme for synthesizing attractors of dissipative chaotic systems," *Appl. Math. Comput.* **201**, 650-667.

D'Aniello, E. & Oliveira, H. [2009] "Pitchfork bifurcation for non-autonomous interval maps," *J. Diff. Eqs. Appl.* **15**, 291-302.

D'Aniello, E. & Steele, T. H. [2011] "The ω-limit sets of alternating systems," *J. Diff. Eqs. Appl.* **17**, 1793-1799.

Maier, M. P. & Peacock-Lopez, E. [2010] "Switching induced oscillations in the logistic map," *Phys. Lett. A* **374**, 1028-1032.

Romera, M., Pastor, G., Martin, A., Orue, A. B., Montoya, F. & Danca, M.-F. [2015] "Breaking Points in Quartic Maps," *Int. J. Bifurcation and Chaos* **25**, 1550051.

Jánosi, I. M. & Gallas, J. A. C. [1999] "Globally coupled multiattractor maps: Mean field dynamics controlled by the number of elements," *Phys. Rev. E* **59**, R28-R31.

Gallas, J. A. C. [1993] "Degenerate routes to chaos," *Phys. Rev. E* **48**, R4156-R4159.

Gallas, J. A. C. [1994] "A method for studying stability domains in physical models," *Physica A* **211**, 57-83.

Gallas, J. A. C. [1995] "Structure of the parameter space of a ring cavity," *Appl. Phys. B* **60**, S203-S213.

Grossmann, S. & Thomae, S. [1977] "Invariant distributions and stationary correlation functions of one-dimensional discrete processes," *Z. Naturforsch A* **32**, 1353-1363.

Milnor, J. & Thurston, W. [1988] "On iterated maps of the interval," *Dynamical Systems*, Lecture Notes in Mathematics, Vol. 1342, pp. 465-563.

Pastor, G., Romera, M. & Montoya, F. [1997] "A revision of the Lyapunov exponent in 1D quadratic maps," *Physica D* **107**, 17-22.

Shaw, R. [1981] "Strange attractors, chaotic behavior and information flow," *Z. Naturforsch A* **36**, 80-112.

Zeng, W.-Z., Hao, B.-L., Wang, G.-R., & Chen, S.-G. [1984] "Scaling property of period-n-tupling sequences in one-dimensional mappings," *Commun. Theor. Phys.* **3**, 283-295.